International Journal of Scientific Research and Reviews

Investigation of Electron Density and Electrical Conductivity of Dicyclopentyl-Cycloh\exane Molecular Nanowire Via Quantum Chemical Calculations

Jayalakshmi P.[1], Meenashi R.[2], Jothi B.[1], Selvaraju K.[3*] and Stephen A. David [4]

[1]Department of Physics, Kandaswami Kandar's College,Velur 638182 Tamilnadu, India,
Email: manijaya2003@gmail.com, Mobile:9487167702
Email: jothiphysics07@gmail.com, Mobile:9488574465
[2]Department of Physics, Kandaswami Kandar's College (UAC),Velur 638182 Tamilnadu, India,
Email: rmeenashi@gmail.com
[3*]Department of Physics, Kandaswami Kandar's College, Velur 638182 Tamilnadu, India,
Email: physicsselvaraj@gmail.com, Mobile:9442430003
[4]Department of Physics, Sri Shakthi Institute of Engineering and Technology, Coimbatore 641062
Tamilnadu, India, Email: davidstephen_dav@yahoo.co.in, Mobile:9952273932

ABSTRACT

The electrical characteristics of gold and sulphur substituted DCC molecular nanowire under the external applied electric field from 0 $V\text{Å}^{-1}$ to 0.26 $V\text{Å}^{-1}$ was investigated from density functional theory (DFT). The structural variation is found to be significant for Au-S bonds for the applied electric field and the mid-portion of DCC molecular nanowire remains unaffected. The bond topological analysis was carried out for all the (3,-1) bond critical points; the systematic variations were noted when the electric field is increased from 0 $V\text{Å}^{-1}$ to 0.26 $V\text{Å}^{-1}$. The nonlinear electrical behavior of DCC nanowire was validated from V-I characteristics.

KEYWORDS: Nanoelectronics; Quantum Calculations; QTAIM theory; I-V characteristics

Corresponding Author:

K. Selvaraju

Assistant Professor and Head,

Department of Physics,

Kandaswami Kandar's College,Velur -638182 Tamilnadu, India.

Email: physicsselvaraj@gmail.com

Mobile: 9442430003

INTRODUCTION

The computational and the trial investigation have given an agreeable exertion for the creation of better leading atoms utilizing to produce the nanoelectronic gadgets. The associations between the components of all nano-electronic parts are shaped with sub-atomic wires. As of late, a few natural atoms were incorporated and their electrical qualities have been contemplated[1]. The electrical conductivity of a sub-atomic wire basically relies upon the sub-atomic structure, its orientation, and the electronenergy density as well as energy density distribution. The configuration of the molecular wire can be distinguished from the manufacturing procedures and connections of anode or cathode for electrical coupling and bond stability. The dicy Clopentylcyclohexane (DCC) systems established the proficient electronic pairing between donor and acceptor in nano-electronic devices. The DCC system possesses excellent electron transport properties[2]. The effective charge transport through the molecule results from the small energy gap between lowest unoccupied molecular orbital (LUMO) and the highest occupied molecular orbital (HOMO) of DCC, and thus, it behaves as an improved molecular nano-wire. The difficulty in understanding the science of charge transport between metal and molecule comesfrom experimental factors and this was overwhelmed from the theoretical electron density analysis via the quantum theory of atoms in molecules (QTAIM).
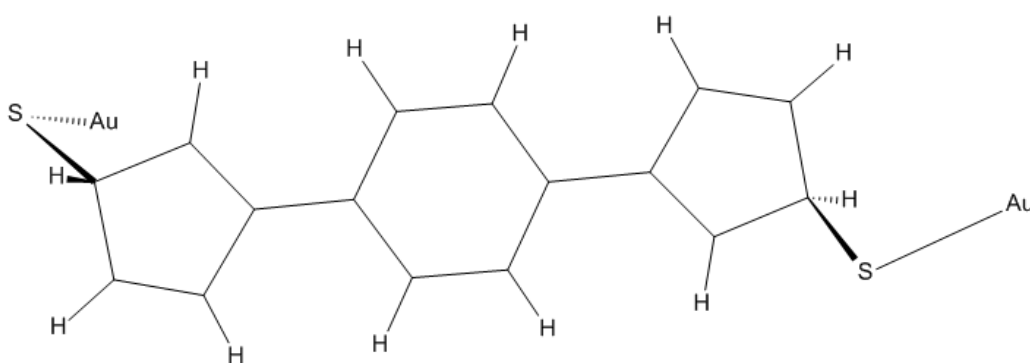

Figure. 1 - Au and S substituted Dicyclopentyl-Cyclohexane molecule.

The topology of electron density and the current-voltage characteristics of Au and S substituted DCC molecule (Fig. 1) werestudiedfor five different electric fieldintensities on the basis of theoretical electron density andtotal energy density viahigh-level density functional calculations together with AIM analysis[3]. The electrical conductance in DCC nanowire for the different applied electric field was well exhibited by their I-V characteristics.

COMPUTATIONAL METHODOLOGY

The optimization of Au and thiol-substituted DCCsystemwas carried out for the five different biasing steps from 0.05 to 0.26VÅ^{-1}as a positive field on the left edge and negative field on the right edge of the DCC moleculeusing Density Functional Theory (DFT) calculations incorporatedin Gaussian03 program suite[4]. The computation was carried along with the B3LYP hybrid function (Becke's three parameters exchange function and Lee, Yang and Parr gradient-corrected correlation function) and LANL2DZ (Los Alamos National Laboratory of Double Zeta) as basis set[5]. Berny algorithm was incorporated in all geometry optimizations. The optimization was accomplished with the threshold convergence for maximum force,0.00045au, root mean square (RMS) force,0.0003au, maximum displacement, 0.001auand root mean square (RMS)displacement, 0.0012 au. The convergence on the density matrix [10^{-8} and 10^{-6}] for the RMS and maximum density matrix error between the iterations was requested to perform the self-consistency of the non-interactive wave function.

From AIMPAC suite[6]theelectron density $\rho_{bcp}(r)$, Laplacian of electron density $\nabla^2\rho_{bcp}(r)$, bond ellipticity ε and the eigenvalues λ_i were calculated at the bond critical point for differentelectric fields. DENPROP and wfn2plots were used for generating thetwo and three-dimensional grids for visualizing the Laplacian of charge density and the deformation density maps.GVIEW packageis used to view the 3D surface plots of molecular frontier orbitals and electrostatic potential. The density of states (DOS) of the molecular nanowire resulted from Gauss Sum program[7].

RESULTS AND DISCUSSION

Geometrical analysis

Lately, the geometrical and topological properties of different molecules have been investigatedin the different applied electric field using DFT[25] method. The geometrically optimized DCC molecular wires for the zero and non-zero applied electric fields were depicted in the Fig. 2. TheDCC has onecentral aromatic ring and at the ends of the molecule, Au atoms were attached through the sulphur atoms. The thiol atom provides betterlinkageof conjugated DCCwith the Au atom[8]. The electrically conducting molecular wires are goodrespondent to the external applied electric field. This often results in the alterationsin the geometrical conformation of the molecules and leads to significantvariation in the electrical conductivityproperties of the molecules[9]. Thus it is more important to compare the zero field geometry against the applied fields to realize the molecular stability over the series of the applied electric field.
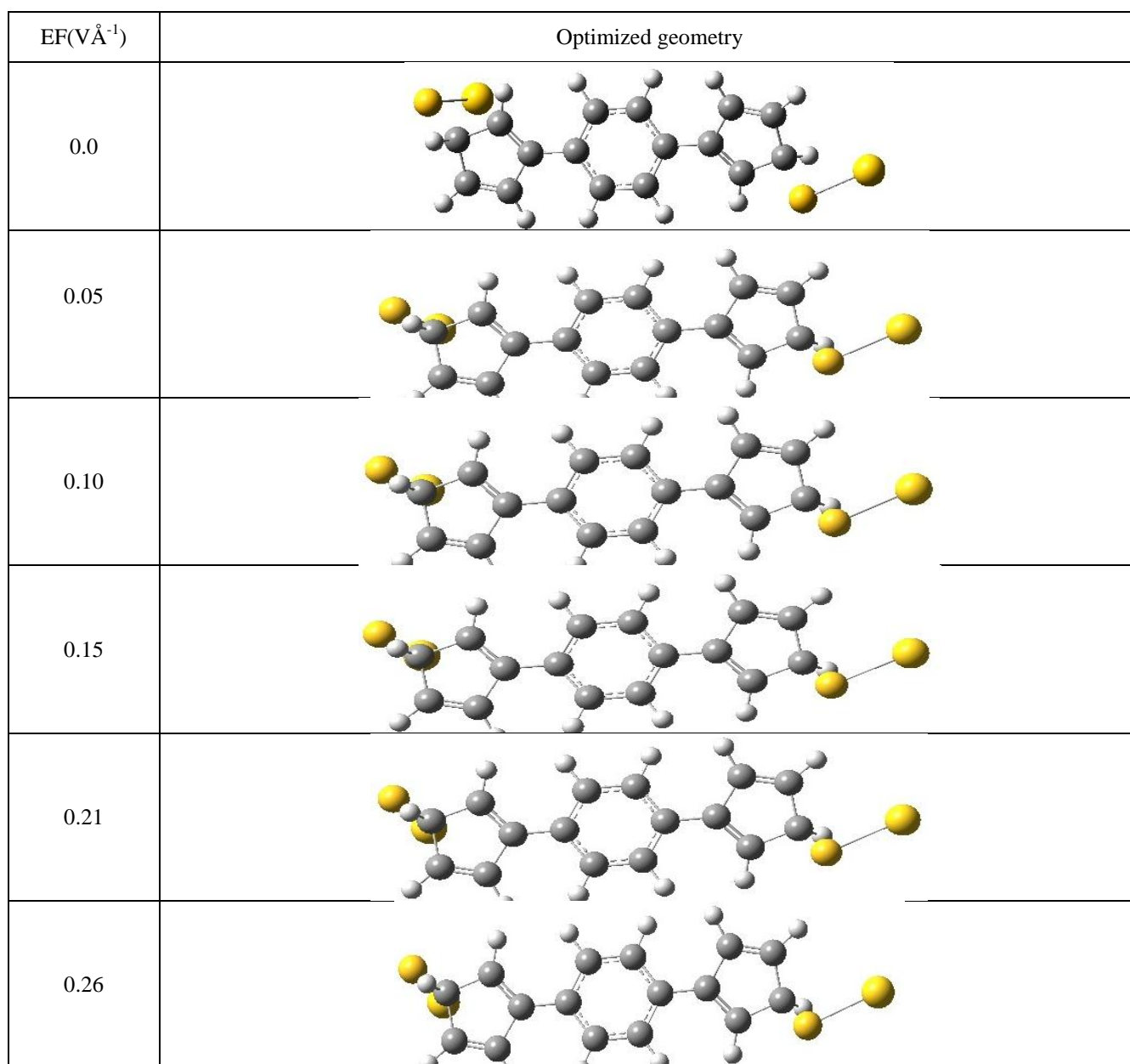
EF(VÅ^{-1})	Optimized geometry
0.0	
0.05	
0.10	
0.15	
0.21	
0.26	

Figure. 2 - Optimized configuration of Au and S substituted DCCmoleculewith the zero and non-zero applied electric field.

On observing the three ring structures (cyclopentane and cyclohexane) under applied field and zero field effects, the C−C bond distances in the molecule varies from 1.360 to 1.514 Å, the maximum perceived variation is 0.008 Å.As the field increases the connector bond C-C distances is decreased from ~1.474 to ~1.467 Å. The S−C bond lengths at zero fieldareabout 1.930 Å; as an increase in the applied electric field, these distances are decreased with a maximum variation of 0.0045 Å. The distance decreased from 1.925 to 1.923 Å, in the L-end, while it is shortened from 1.935 to 1.931 Åin the R-end;the variations [~ 0.02Å] are found to be equal in the both R-end and L-end.The Au−S bond distances are found unequal for the zero and the applied field. In the R-end, Au-S bond distance was found to be increased from 2.391 to 2.427 Å as the field increases; notably, there is no variationwas observed in L-end of the DCC molecular wire for all the applied electric

fields. The Au-S distances at L- and R-ends are computed as 2.386 and 2.427 Å for the maximum applied field (0.26 VÅ^{-1}). This hugevariance is endorsed to the applied electric field increasing the Au−S bond distance over by attenuating the S−C bond length in DCC molecular wire (Table 1).However, theC−H bond lengths were found to be almost equal [1.086 Å] for all the applied electric field. Table.1explores the complete spectrum of bond distance values of Au and S substituted DCC molecule for the zero and higher applied electric fields.

Table No. 1:"Bond distances (Å) of Au and S substituted DCC molecular wire for the zero andhigher applied EFs (VÅ^{-1})"

Bonds	Applied electric field (VÅ^{-1})					
	0	0.05	0.10	0.15	0.21	0.26
Ring 1						
C(3)-C(2)	1.372	1.372	1.372	1.373	1.375	1.377
C(3)-C(4)	1.493	1.493	1.492	1.492	1.491	1.49
C(2)-C(1)	1.508	1.508	1.507	1.507	1.505	1.504
C(1)-C(5)	1.514	1.514	1.513	1.513	1.512	1.512
C(5)-C(4)	1.36	1.36	1.36	1.36	1.361	1.362
Ring 2						
C(7)-C(6)	1.417	1.418	1.418	1.419	1.421	1.422
C(7)-C(8)	1.399	1.399	1.398	1.398	1.396	1.396
C(6)-C(11)	1.418	1.419	1.419	1.42	1.422	1.423
C(10)-C(9)	1.417	1.417	1.417	1.418	1.419	1.421
C(9)-C(8)	1.419	1.419	1.419	1.42	1.421	1.423
C(10)-C(11)	1.399	1.399	1.398	1.398	1.396	1.396
Ring 3						
C(12)-C(13)	1.489	1.489	1.489	1.489	1.489	1.489
C(12)-C(16)	1.375	1.376	1.378	1.38	1.383	1.385
C(13)-C(14)	1.36	1.36	1.36	1.36	1.36	1.36
C(14)-C(15)	1.511	1.511	1.511	1.511	1.511	1.511
C(15)-C(16)	1.509	1.508	1.508	1.507	1.506	1.505
Ring Connectors						
C(6)-C(3)	1.475	1.475	1.474	1.473	1.471	1.469
C(9)-C(12)	1.474	1.473	1.471	1.469	1.467	1.465
Terminal						
C(15)-S(2)	1.935	1.935	1.934	1.933	1.932	1.931
C(1)-S(1)	1.925	1.924	1.923	1.923	1.923	1.924
S(2)-Au(2)	2.391	2.394	2.398	2.405	2.414	2.427
S(1)-Au(1)	2.385	2.385	2.385	2.384	2.386	2.386
C-H Bonds						
C(1)-H(1)	1.101	1.101	1.101	1.101	1.101	1.101
C(2)-H(2)	1.083	1.083	1.083	1.083	1.083	1.083
C(4)-H(4)	1.084	1.084	1.084	1.084	1.084	1.084
C(5)-H(5)	1.083	1.083	1.083	1.083	1.083	1.083
C(7)-H(7)	1.087	1.087	1.087	1.086	1.086	1.086
C(10)-H(10)	1.087	1.087	1.087	1.087	1.087	1.087
C(8)-H(8)	1.087	1.087	1.087	1.087	1.087	1.087
C(13)-H(13)	1.084	1.084	1.084	1.084	1.084	1.084
C(14)-H(14)	1.083	1.084	1.084	1.084	1.084	1.084
C(16)-H(16)	1.083	1.083	1.083	1.083	1.083	1.083

There is no any significant difference was noticed in the bond angles of the DCC wire when compared the values for applied field against the zero field. Similarly, the applied electric field leads to no significant difference in the bond angles of the terminal (C−C−S and Au−S−C) bonds. Specifically, for the zero field and the higher field, the C−C−S bond angle is ~114.5 and ~114.25°respectively. Furtherwith the increase of fieldfrom zero to the higher electric field, the Au−S−C bond angles are found to be increased by 1° and the maximum angle is found at 0.26 VÅ^{-1} [~103.5°].Further, the C−C−C bond angles (~109.77°)at cyclopentanerings almost remain the same with the increase of field from 0VÅ^{-1}and for cyclohexane, it is observed to be (~121.2°) [Table 2] whichalso remains same with the increase of the field.

Table No. 2:"Bond angles (°) of Au and S substituted DCC molecular wire for the zero and higher applied EFs (VÅ^{-1})"

Bonds	Applied Electric Field(VÅ^{-1})					
	0	0.05	0.1	0.15	0.21	0.26
Ring 1						
C(2)-C(3)-C(4)	107.9	107.9	107.9	107.9	107.8	107.8
C(3)-C(2)-C(1)	109.8	109.7	109.7	109.7	109.8	109.8
C(2)-C(1)-C(5)	103.6	103.6	103.6	103.6	103.6	103.6
C(1)-C(5)-C(4)	108.9	108.9	109	109	109	109.1
C(3)-C(4)-C(5)	109.8	109.8	109.7	109.7	109.7	109.7
Ring 2						
C(6)-C(7)-C(8)	121.3	121.3	121.3	121.3	121.4	121.4
C(7)-C(6)-C(11)	117.4	117.4	117.4	117.4	117.3	117.2
C(7)-C(6)-C(3)	121.4	121.4	121.4	121.4	121.4	121.5
C(11)-C(6)-C(3)	121.1	121.1	121.2	121.2	121.3	121.3
C(6)-C(11)-C(10)	121.3	121.3	121.3	121.3	121.4	121.4
C(11)-C(10)-C(9)	121.2	121.2	121.2	121.2	121.2	121.3
C(10)-C(9)-C(8)	117.5	117.5	117.5	117.5	117.4	117.4
C(7)-C(8)-C(9)	121.3	121.2	121.3	121.3	121.3	121.3
Ring 3						
C(13)-C(12)-C(16)	108	107.9	107.9	107.8	107.7	107.6
C(12)-C(13)-C(14)	109.7	109.7	109.8	109.8	109.8	109.9
C(13)-C(14)-C(15)	109.2	109.2	109.2	109.2	109.2	109.2
C(14)-C(15)-C(16)	103.5	103.5	103.5	103.6	103.6	103.6
C(12)-C(16)-C(15)	109.6	109.6	109.7	109.7	109.7	109.7
Ring Connectors						
C(6)-C(3)-C(2)	127.6	127.5	127.3	127.2	127	126.8
C(6)-C(3)-C(4)	124.5	124.6	124.7	124.9	125.2	125.4
C(10)-C(9)-C(12)	121.4	121.4	121.5	121.5	121.6	121.7
C(8)-C(9)-C(12)	121.1	121	121	121	121	120.9
C(9)-C(12)-C(13)	124.5	124.5	124.4	124.4	124.4	124.4
C(9)-C(12)-C(16)	127.5	127.6	127.7	127.8	127.9	127.9
Terminal						
C(14)-C(15)-S(2)	112.7	112.6	112.4	112.3	112.3	112.3
C(16)-C(15)-S(2)	106.1	105.8	105.4	104.9	104.4	104.2
C(2)-C(1)-S(1)	114.6	114.5	114.3	114.1	113.6	113.1
C(5)-C(1)-S(1)	114.4	114.6	114.8	115	115.3	115.4
C(15)-S(2)-Au(2)	102.8	102.9	103.1	103.4	103.8	104.1
C(1)-S(1)-Au(1)	101.2	101.6	101.9	102.3	102.6	103

The applied field made an appreciable increase in the torsion angle of the C−C−C−C ring bonds as well as the spine bonds of the molecule; the maximum difference of torsion angle 0.6° is observed when the field increased from 0 to 0.26 VÅ^{-1}. For the zero field, the torsion angles S–C–C–C bonds in the right end is ~118.9° and the left end shows the angle of ~126.8°; with an increase in the field, this angle is decreasedby ~0.1°. While Au–S–C–C bonds in both the left and right end shows an appreciable increase in bond twit as the field increases. The zero field torsion angle of left end Au–S–C–C bond is 60.1°; as the field increases, this angle gradually increases to 73.6°(0.26VÅ^{-1})with the increase of field, whereas the right end torsion angle at zero fields is -59.4° which is decreased to -45.4°with the field increases.
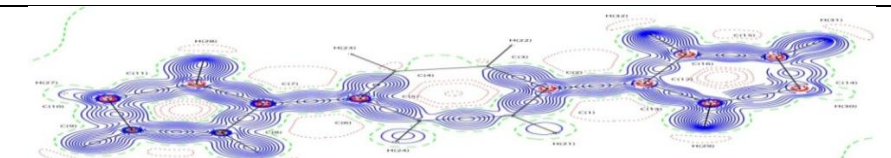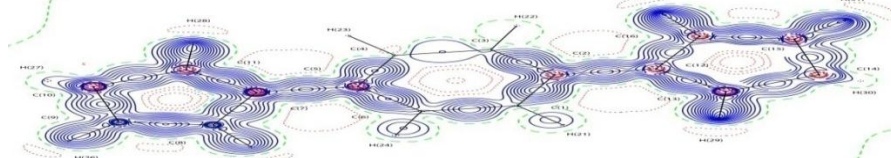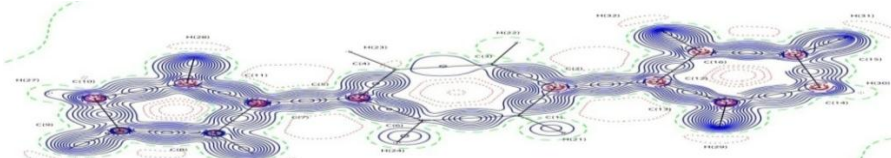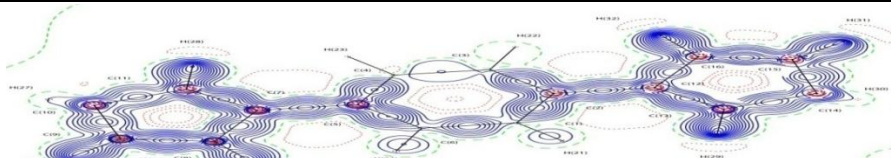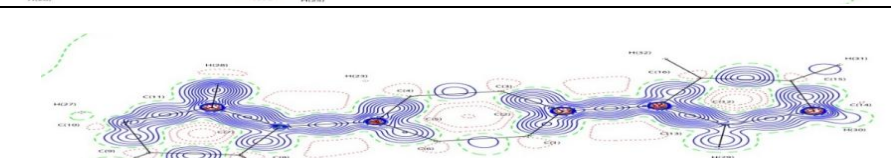
Overall, on the application of the external electric field, the variations at the central region of the DCC molecular wire remain the same. Specifically, there is a wide variation is noticed in the terminal groups between the ends of the molecule [Table 3]. Thus the structural evaluationfor different fields reveals that, comparatively, the terminal groups are found to be highly reactive to the applied electric field.

Table No. 3:"Torsion angles (°) of Au and S substituted DCC molecular wire for the zero and higher applied EFs (VÅ^{-1})"

Bonds	Applied Electric Field(VÅ^{-1})					
	0	**0.05**	**0.1**	**0.15**	**0.21**	**0.26**
Ring 1						
C(4)-C(3)-C(2)-C(1)	0.6	0.6	0.5	0.5	0.5	0.4
C(2)-C(3)-C(4)-C(5)	0.3	0.3	0.3	0.4	0.3	0.3
C(3)-C(2)-C(1)-C(5)	-1.1	-1.1	-1.1	-1.1	-1	-0.9
C(2)-C(1)-C(5)-C(4)	1.3	1.3	1.3	1.3	1.2	1.1
C(1)-C(5)-C(4)-C(3)	-1	-1	-1.1	-1.1	-0.9	-0.9
C(6)-C(3)-C(2)-C(1)	-179.5	-179.5	-179.4	-179.3	-179.1	-178.9
C(6)-C(3)-C(4)-C(5)	-179.7	-179.7	-179.7	-179.8	179.9	179.7
Ring 2						
C(8)-C(7)-C(6)-C(11)	-0.4	-0.4	-0.4	-0.4	-0.4	-0.2
C(8)-C(7)-C(6)-C(3)	179	179	179.1	179.1	179.1	179.1
C(6)-C(7)-C(8)-C(9)	0.4	0.5	0.5	0.5	0.5	0.5
C(7)-C(6)-C(11)-C(10)	0.4	0.3	0.3	0.2	0.1	0
C(3)-C(6)-C(11)-C(10)	-179.1	-179.1	-179.2	-179.2	-179.3	-179.4
C(10)-C(9)-C(8)-C(7)	-0.3	-0.3	-0.4	-0.4	-0.4	-0.5
C(6)-C(11)-C(10)-C(9)	-0.3	-0.3	-0.2	-0.2	-0.1	0
C(11)-C(10)-C(9)-C(8)	0.3	0.2	0.2	0.2	0.2	0.2
Ring 3						
C(13)-C(12)-C(16)-C(15)	0.3	0.2	0.2	0.1	0	-0.2
C(12)-C(13)-C(14)-C(15)	0.8	0.8	0.8	0.8	0.7	0.7
C(13)-C(14)-C(15)-C(16)	-0.6	-0.7	-0.7	-0.7	-0.7	-0.8
C(16)-C(12)-C(13)-C(14)	-0.7	-0.7	-0.6	-0.5	-0.4	-0.3
Ring Connectors						
C(7)-C(6)-C(3)-C(2)	-14.4	-14.8	-14.9	-14.5	-12	-11.6
C(7)-C(6)-C(3)-C(4)	165.5	165.1	165.1	165.7	168.4	169.1
C(11)-C(6)-C(3)-C(2)	165	164.6	164.6	165	167.4	167.7
C(11)-C(6)-C(3)-C(4)	-15.1	-15.4	-15.4	-14.8	-12.2	-11.5

C(11)-C(10)-C(9)-C(12)	-179.7	-179.6	-179.4	-179.3	-179.1	-178.8
C(12)-C(9)-C(8)-C(7)	179.6	179.5	179.3	179.1	178.9	178.6
C(10)-C(9)-C(12)-C(13)	-162.2	-162.6	-163.4	-164.4	-164.9	-165.9
C(10)-C(9)-C(12)-C(16)	18.5	18.2	17.8	17.2	17	16.6
C(8)-C(9)-C(12)-C(13)	17.9	17.6	17	16.2	15.8	15.1
C(8)-C(9)-C(12)-C(16)	-161.5	-161.6	-161.9	-162.3	-162.2	-162.4
C(9)-C(12)-C(13)-C(14)	179.8	-180	-179.6	-179.3	-178.8	-178.2
C(9)-C(12)-C(13)-H(13)	2.4	2.7	3	3.4	4	4.6
C(9)-C(12)-C(16)-C(15)	179.8	179.5	179.1	178.8	178.2	177.6
Terminal						
C(13)-C(14)-C(15)-S(2)	-114.7	-114.4	-113.9	-113.3	-112.8	-112.6
C(14)-C(15)-C(16)-C(12)	0.1	0.2	0.3	0.3	0.4	0.6
S(2)-C(15)-C(16)-C(12)	118.9	118.8	118.5	118.3	118.1	118.2
C(14)-C(15)-S(2)-Au(2)	-66.9	-66.4	-66.2	-66.3	-66.6	-67.1
C(16)-C(15)-S(2)-Au(2)	-179.4	-178.7	-178.3	-178.1	-178.2	-178.5
C(3)-C(2)-C(1)-S(1)	-126.5	-126.6	-126.8	-126.9	-126.8	-126.5
S(1)-C(1)-C(5)-C(4)	126.8	126.7	126.7	126.6	125.9	125.2
C(2)-C(1)-S(1)-Au(1)	60.1	61.6	63.1	65.3	71.3	73.6
C(5)-C(1)-S(1)-Au(1)	-59.4	-58	-56.5	-54.3	-48	-45.4

Charge density distribution

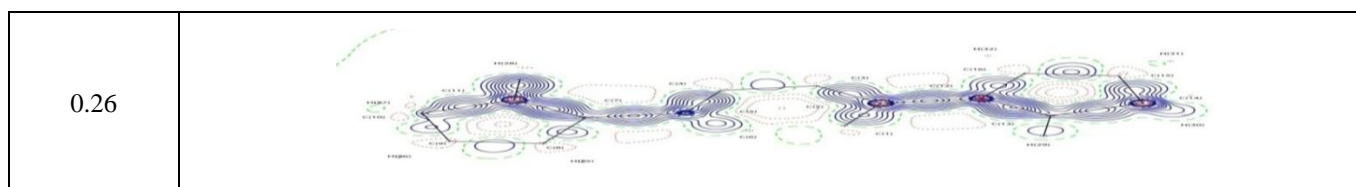| EF $(V\mathring{A}^{-1})$	Deformation density
0.0	
0.05	
0.10	
0.15	
0.21	

| 0.26 | |

Figure. 3 - Deformation density mapsofAu and S substituted DCCforthezero and higher applied electric field.

The association between the topology of electron density at the bond critical points and the chemical conceptscan be well countedfrom Quantum theory of atoms in molecules (QTAIM). The bond topological parameters at bcp of DCC molecular wire for applied electric fields were listed in Table 4. The presence of a chemical bond between the two atoms was authorized from the topological electron densityanalysis. In more specific in our investigation, the Au–S bond embraces, the gold and sulphur interaction is not a covalent type. The positive Laplacian of electron density $\nabla^2\rho(r)$ was noted for Au–S bonds which confirms their *closed-shell*interactions. The similar kind of studies was already reported in Gibbs *et al.*'s and Cremer-Kraka's work [10,11].

The 2-dimensional contour plot of deformation density of the DCC molecule calculated at ring planes for the zero and various applied EFs, obtained from the difference of total aspherical and spherical atom densities are clearly depicted in Fig. 3. Further, it shows the charge concentration at the bond critical point for the zero and higher electric fields. The electron density [$\rho_{bcp}(r)$] at the bcp of all cyclopentyl C−C bonds ranges from 1.60 to 2.10 eÅ^{-3} for the zero field, and these values were found to be reduced slightlyfor higher electric fields; the maximum variation is 0.04 eÅ^{-3}.There is no significant variation in the electron density [$\rho_{bcp}(r)$] at the bcp of all cyclohexane C−C bonds as their average value is1.90 eÅ^{-3} for the applied field. The zero field density $\rho_{bcp}(r)$ of C=C bonds (ring connector) is ~1.73 eÅ$^{-3,}$ the bond densities are found to be almost equal for all the applied fields. At zero field, the S−C bond density is 0.853 eÅ^{-3}, and whentheapplied field increases, it is slightly increased by a maximum of 0.006 eÅ^{-3}. Particularly, the S−C bond electron density is feeble, which shows that the charges of these bonds at the bond critical point migrated away from the inter-nuclear axis, which favorsthe π-bond characteristic. Thesimilar scenario can be reflected from the Laplacian of electron density and the bond ellipticity[10] at the bcp. The electron density of Au−S bond for zero fields is ~0.534 eÅ^{-3}, whereas, for the applied field, the variation is found to be very small in left edge when compared with the right edge of the molecule, as the average electron density value is 0.516eÅ^{-3}. For the zero field, the C−H bond density is ~1.8 eÅ^{-3}, which is almost equal to the field increases (Table 4). There is no much alterations found in the electron density at the bcp's of DCC molecule for zero and applied electric field. The complete spectrum of electron density at (3,-1) regions of Au and S substituted DCC molecule for the zero and higher electric field (VÅ^{-1}) are listed in Table 4.

Table No. 4:"Electron density ρ$_{bcp}$(r) (eÅ^{-3}) values of Au and S substituted DCC molecular wire for the zero and higher applied EFs (VÅ^{-1})"

Bonds	Applied Electric Field (VÅ^{-1})					
	0	0.05	0.01	0.15	0.21	0.26
Ring 1						
C(3)-C(2)	2.06	2.06	2.06	2.06	2.05	2.04
C(3)-C(4)	1.65	1.65	1.65	1.65	1.66	1.66
C(2)-C(1)	1.62	1.62	1.62	1.62	1.63	1.63
C(1)-C(5)	1.6	1.6	1.6	1.6	1.6	1.6
C(5)-C(4)	2.1	2.1	2.1	2.1	2.1	2.09
Ring 2						
C(7)-C(6)	1.9	1.9	1.9	1.9	1.89	1.89
C(7)-C(8)	1.96	1.96	1.96	1.97	1.97	1.97
C(6)-C(11)	1.9	1.9	1.9	1.89	1.89	1.89
C(10)-C(9)	1.9	1.9	1.9	1.9	1.89	1.89
C(9)-C(8)	1.9	1.9	1.89	1.89	1.89	1.88
C(8)-H(8)	1.79	1.79	1.79	1.79	1.79	1.79
Ring 3						
C(12)-C(13)	1.67	1.67	1.67	1.67	1.67	1.67
C(12)-C(16)	2.05	2.04	2.04	2.03	2.02	2.01
C(13)-C(14)	2.1	2.1	2.1	2.1	2.1	2.1
C(14)-C(15)	1.61	1.61	1.61	1.61	1.61	1.61
C(15)-C(16)	1.61	1.61	1.61	1.61	1.61	1.62
Ring Connectors						
C(6)-C(3)	1.71	1.71	1.72	1.72	1.73	1.73
C(9)-C(12)	1.72	1.72	1.73	1.73	1.74	1.75
Terminal						
C(15)-S(2)	0.844	0.846	0.847	0.848	0.849	0.85
C(1)-S(1)	0.862	0.864	0.865	0.865	0.862	0.861
S(2)-Au(2)	0.53	0.526	0.522	0.515	0.506	0.494
S(1)-Au(1)	0.537	0.537	0.537	0.537	0.536	0.536
C-H Bonds						
H(1)-C(1)	1.72	1.72	1.72	1.72	1.72	1.72
C(2)-H(2)	1.79	1.79	1.79	1.8	1.8	1.8
C(4)-H(4)	1.79	1.79	1.79	1.79	1.79	1.79
C(5)-H(5)	1.8	1.8	1.8	1.8	1.8	1.81
C(7)-H(7)	1.79	1.79	1.79	1.8	1.8	1.8
C(10)-H(10)	1.79	1.79	1.79	1.79	1.79	1.79
C(11)-H(11)	1.79	1.79	1.8	1.8	1.8	1.8
C(13)-H(13)	1.79	1.79	1.79	1.8	1.8	1.8
C(14)-H(14)	1.79	1.79	1.79	1.79	1.79	1.79
C(15)-H(15)	1.761	1.762	1.763	1.764	1.764	1.763
C(16)-H(16)	1.79	1.79	1.79	1.79	1.79	1.79

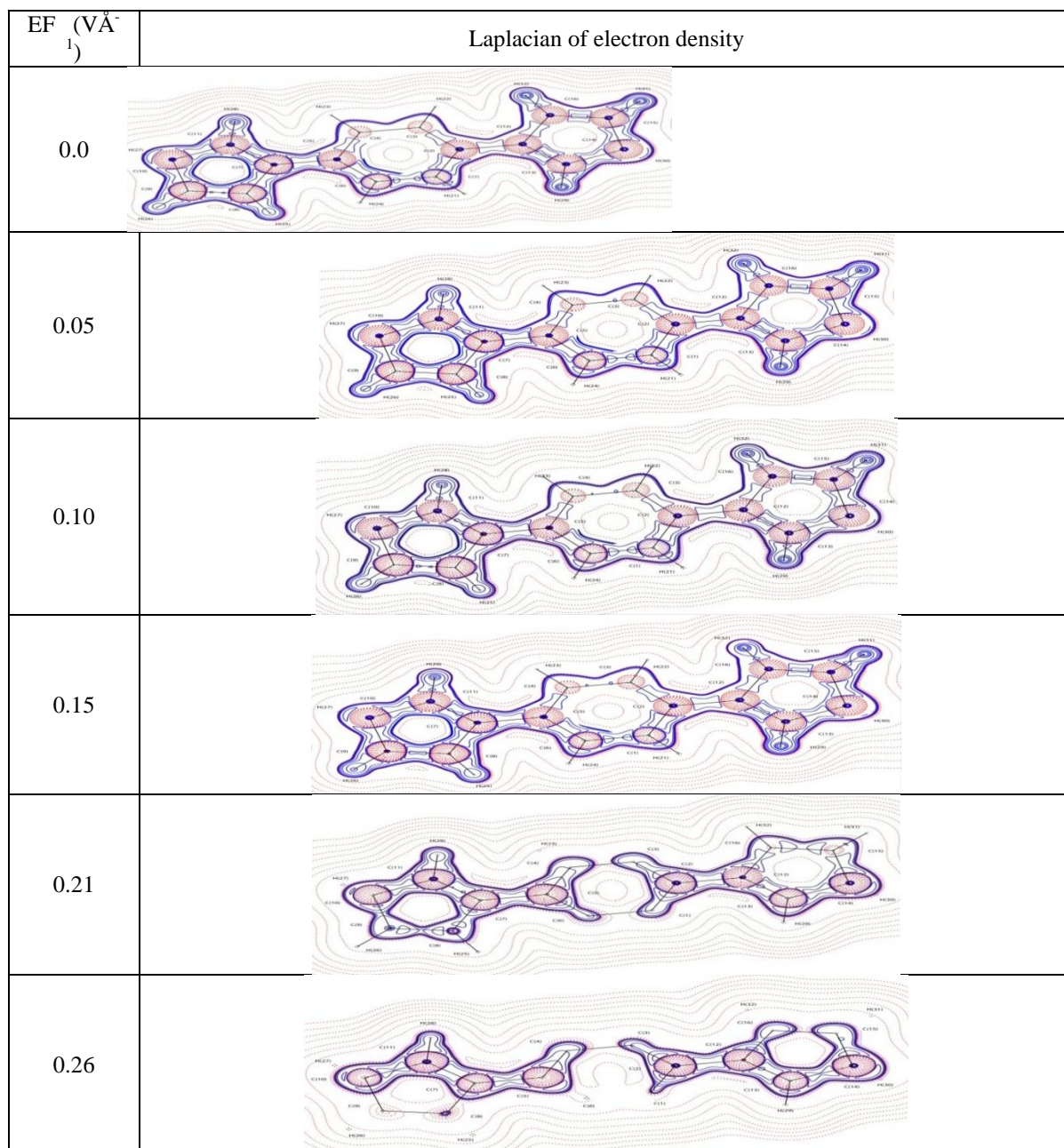| EF (VǺ$^{-1}$)	Laplacian of electron density
0.0	
0.05	
0.10	
0.15	
0.21	
0.26	

Figure. 4 - The contour plot of the Laplacian of electron density maps of the DCC molecule for the zero and various applied EFs.

The charge accumulation or depletion of covalent and non-covalent bonds was well established from the Laplacian of electron density $[\nabla^2\rho_{bcp}(r)]$ at the bcp. The variation of Laplacian of electron density at the bcp of all bonds in the molecule has been noted for the applied external electric field. Table 5 shows the predictedLaplacian of electron density for five levels of the applied electric field. Fig. 4 displaystheLaplacian of electron density for the zero and non-zero higher applied electric fields (VǺ$^{-1}$).

The projected Laplacian of electron density for the cyclohexane C−C bonds are ~-17.8 eÅ^{-5} for zero applied field; when the field increases, these values are come to be a little negative, specifies, the charges in the bcpof these bonds are marginally depleted. For the cyclopentyl rings, the $\nabla^2\rho_{bcp}(r)$ values of C-C bonds at zero field ranges from -11.9 to -20.8 eÅ^{-5} and there is no significant variation for the increased fields. A similar trend also found in the C=C (ring connector) of the DCC, where the Laplacian for zero fields is ~-14.6 eÅ^{-5}; for the applied field, these values were slightly increased by the maximum of 0.4 eÅ^{-5}. The Laplacian$\nabla^2\rho_{bcp}(r)$for C−H bonds ranges from -19.1 to -20.8 eÅ^{-5} for the zero electric field, this high negative value that the charges of the bonds are extremely accumulated, and these values are reformed withthe maximum variation of 0.4 eÅ^{-5} when the applied field increases. The charges in S-C bonds ~-2.0 eÅ^{-5}at the left end of the molecule, this value is found to be decreased to ~ -1.8 eÅ^{-5} and at the right end. The dissimilarity designates that the charges at the left end are faintly accumulated than at the right end. For the zero field, the Laplacian of electron density of Au−S bond is found to be ~2.94 eÅ^{-5}, as the field increases, this value increases abruptly at the left end (3.07 eÅ^{-5}) and the trend at theright end slightly decreases (2.85 eÅ^{-5}). The zero field Laplacian of C−H bonds (~-20.3eÅ^{-5}), differ marginally with the increase of the applied electric field. On the whole, the Laplacian of electron density distribution $\nabla^2\rho_{bcp}(r)$in Au−S−DCC−S−Au, discloses that the applied electric field makes the charges to be depleted at the bcps of C−C and C=C bonds, whereas this influence is found to be slightly enhanced in the terminal bonds, precisely it is high at the left end. The predictedLaplacianvalues of Au and S substituted DCC molecular wire for zero and higher applied fields are listed in Table 5.

Table No. 5:"Laplacian of electron density $\nabla^2\rho_{bcp}(r)$(eÅ^{-5}) valuesof Au and S substituted DCC molecular wire for the zero and higher applied EFs (VÅ^{-1})"

Bonds	Applied electric field					
	0	0.05	0.1	0.15	0.21	0.26
Ring 1						
C(3)-C(2)	-20	-20	-20	-19.9	-19.9	-19.7
C(3)-C(4)	-13	-13	-13	-13	-13.1	-13.1
C(2)-C(1)	-12.2	-12.3	-12.3	-12.4	-12.5	-12.6
C(1)-C(5)	-11.9	-12	-12	-12	-12	-12.1
C(5)-C(4)	-20.8	-20.7	-20.7	-20.7	-20.7	-20.7
Ring 2						
C(7)-C(6)	-17.6	-17.6	-17.6	-17.5	-17.5	-17.4
C(7)-C(8)	-18.7	-18.7	-18.7	-18.8	-18.9	-18.9
C(6)-C(11)	-17.5	-17.5	-17.5	-17.5	-17.4	-17.4
C(10)-C(9)	-17.6	-17.6	-17.6	-17.5	-17.5	-18.8
C(9)-C(8)	-17.5	-17.5	-17.4	-17.4	-17.3	-17.3
Ring 3						
C(12)-C(13)	-13.2	-13.3	-13.3	-13.3	-13.3	-13.4
C(12)-C(16)	-19.8	-19.7	-19.6	-19.5	-19.3	-19.2

C(13)-C(14)	-20.8	-20.8	-20.8	-20.8	-20.8	-20.8
C(14)-C(15)	-12.1	-12.1	-12.1	-12.1	-12.1	-12.1
C(15)-C(16)	-12.1	-12.1	-12.1	-12.2	-12.2	-12.3
Ring Connectors						
C(6)-C(3)	-14.5	-14.6	-14.6	-14.7	-14.8	-14.9
C(9)-C(12)	-14.7	-14.7	-14.8	-14.9	-15	-15.1
Terminal						
C(15)-S(2)	-1.806	-1.806	-1.804	-1.8	-1.797	-1.798
C(1)-S(1)	-2.007	-2.03	-2.046	-2.056	-2.037	-2.019
S(2)-Au(2)	2.898	2.868	2.846	2.834	2.836	2.851
S(1)-Au(1)	2.988	2.99	2.996	3.009	3.035	3.074
C-H Bonds						
H(1)-C(1)	-19.1	-18.7	-18.8	-18.8	-18.9	-19.1
C(2)-H(2)	-20.6	-20.6	-20.7	-20.7	-20.8	-20.9
C(4)-H(4)	-20.5	-20.5	-20.4	-20.4	-20.4	-20.4
C(5)-H(5)	-20.8	-20.9	-21	-21.1	-21.2	-21.4
C(7)-H(7)	-20.3	-20.4	-20.5	-20.5	-20.6	-20.7
C(8)-H(8)	-20.3	-20.3	-20.2	-20.2	-20.2	-20.2
C(10)-H(10)	-20.4	-20.3	-20.3	-20.3	-20.2	-20.2
C(11)-H(11)	-20.3	-20.4	-20.4	-20.5	-20.6	-20.6
C(13)-H(13)	-20.5	-20.6	-20.7	-20.7	-20.8	-20.8
C(14)-H(14)	-20.7	-20.7	-20.6	-20.6	-20.6	-20.5
C(15)-H(15)	-19.811	-19.808	-19.805	-19.801	-19.785	-19.742
C(16)-H(16)	-20.5	-20.5	-20.6	-20.6	-20.6	-20.6

The bond ellipticity $\varepsilon = (\lambda_1/\lambda_2)-1$, can be calculated to determine the anisotropy of charge density distribution at the bond critical point of molecules, where λ_1 and λ_2 are the negative eigenvalues of Hessian matrix. The anisotropic behavior of bonding density results thedurable deviations from σ-type bond nature; this was well reflected from the high ellipticity values. Theaverage value of ellipticity for cyclohexane C−C bonds [0.13] is found little less when compared with that of cyclopentyl rings and the values are around 0.12. As the field increases, the bond ellipticity of C−C bond at connection part also increases gradually from 0.056 to 0.068. With the increase in the applied electric field the bond ellipticity of S−C bond at the left end increases progressively from 0.08 to 0.083, conversely, and at the right end, the ellipticity value decreases from 0.097 to 0.090. Au−S bonds have relatively high εvalue [~0.1], for the increase of field and this proves that the charges are highly anisotropy and they are listed in Table 6.

Table No. 6:"Bond ellipticity valuesof Au and S substituted DCC molecular wire for the zero and higher applied EFs (VÅ⁻¹)"

Bonds	Applied electric field (VÅ⁻¹)					
	0	0.05	0.1	0.15	0.21	0.26
Ring 1						
C(3)-C(2)	0.239	0.237	0.233	0.229	0.221	0.211
C(3)-C(4)	0.058	0.06	0.062	0.064	0.065	0.067
C(2)-C(1)	0.037	0.036	0.036	0.035	0.034	0.033
C(1)-C(5)	0.029	0.029	0.029	0.029	0.029	0.028
C(5)-C(4)	0.248	0.247	0.247	0.246	0.244	0.241
Ring 2						
C(7)-C(6)	0.134	0.132	0.129	0.126	0.122	0.119
C(7)-C(8)	0.153	0.153	0.153	0.154	0.155	0.132
C(6)-C(11)	0.134	0.132	0.129	0.126	0.122	0.119
C(10)-C(9)	0.136	0.137	0.137	0.136	0.134	0.132
C(9)-C(8)	0.134	0.135	0.135	0.134	0.132	0.13
Ring 3						
C(12)-C(13)	0.059	0.057	0.055	0.054	0.053	0.053
C(12)-C(16)	0.231	0.229	0.225	0.22	0.215	0.21
C(13)-C(14)	0.246	0.245	0.244	0.243	0.242	0.241
C(14)-C(15)	0.024	0.023	0.023	0.023	0.022	0.022
C(15)-C(16)	0.037	0.038	0.039	0.039	0.04	0.04
Ring Connectors						
C(6)-C(3)	0.058	0.058	0.058	0.059	0.061	0.063
C(9)-C(12)	0.056	0.058	0.06	0.062	0.065	0.068
Terminal						
C(15)-S(2)	0.097	0.096	0.094	0.093	0.091	0.09
C(1)-S(1)	0.08	0.08	0.082	0.083	0.084	0.083
S(2)-Au(2)	0.101	0.102	0.102	0.103	0.102	0.102
S(1)-Au(1)	0.099	0.099	0.099	0.099	0.098	0.096
C-H Bonds						
C(1)-H(1)	0.007	0.006	0.005	0.004	0.004	0.004
C(2)-H(2)	0.013	0.011	0.009	0.007	0.005	0.004
C(4)-H(4)	0.004	0.005	0.006	0.007	0.007	0.007
C(5)-H(5)	0.008	0.007	0.007	0.006	0.005	0.004
C(7)-H(7)	0.004	0.004	0.004	0.004	0.004	0.004
C(10)-H(10)	0.003	0.003	0.003	0.003	0.002	0.002
C(11)-H(11)	0.004	0.004	0.004	0.004	0.004	0.004
C(13)-H(13)	0.005	0.005	0.004	0.004	0.004	0.004
C(14)-H(14)	0.007	0.007	0.008	0.008	0.008	0.008
C(15)-H(15)	0.007	0.008	0.008	0.009	0.009	0.009
C(16)-H(16)	0.016	0.017	0.018	0.018	0.019	0.019

Energy density

Chemical interactionswerealso investigatedfrom energetic and electrostatic aspects of chemical bonds in molecules. In the present study, the total energy density distribution of DCC molecule has been predicted, which is associatedwith Laplacian of electron density. The total energy density H(r) from potential energy density V(**r**) and the local kinetic energy density G(**r**) can be equated as H(**r**) =

G(**r**) + V(**r**). In the current analysis, the G(**r**) is positive, V(**r**) is negative and the total energy density H(**r**) is negative, it is obvious that V(**r**) always dominates for all cases.

Comparatively, the total energy density H(**r**) for the C-C bonds of cyclohexane ring is high (~-1.862 HÅ^{-3}) for zero fields among the other bonds in the molecule; this value was marginally decreased to ~ -1.848 HÅ^{-3}for the applied higher field. The similar trend was reflected in the cyclopentyl ring C–C and C–H bonds, where the total energy density values are ~-1.685and ~-1.713HÅ^{-3}respectively. From the table 7, it was cleared that the magnitude of the total energy density of Au–S and S–C bonds are considerably less when compared with other bonds in the DCC molecular wire. The total energy density H(r) of Au–S and S–C bonds differs from -0.143 to -0.166 HÅ^{-3} and -0.393 to -0.418 HÅ^{-3} respectively for the applied electric field.

Table No. 7:"Bond energy density H(r) (HÅ^{-3}) values of Au and S substituted DCC molecular wire for the zero and higher applied EFs (VÅ^{-1})"

Bonds	Applied electric field(VÅ^{-1})					
	0	0.05	0.1	0.15	0.21	0.26
Ring 1						
C(3)-C(2)	-2.17	-2.17	-2.17	-2.16	-2.15	-2.13
C(3)-C(4)	-1.37	-1.37	-1.37	-1.38	-1.38	-1.39
C(2)-C(1)	-1.3	-1.3	-1.31	-1.31	-1.32	-1.33
C(1)-C(5)	-1.27	-1.27	-1.27	-1.28	-1.28	-1.28
C(5)-C(4)	-2.26	-2.26	-2.26	-2.25	-2.25	-2.24
Ring 2						
C(7)-C(6)	-1.84	-1.84	-1.84	-1.83	-1.82	-1.82
C(7)-C(8)	-1.96	-1.96	-1.97	-1.97	-1.98	-1.99
C(6)-C(11)	-1.83	-1.83	-1.83	-1.82	-1.82	-1.81
C(10)-C(9)	-1.85	-1.84	-1.84	-1.83	-1.83	-1.82
C(9)-C(8)	-1.83	-1.83	-1.83	-1.82	-1.81	-1.8
Ring 3						
C(12)-C(13)	-1.39	-1.39	-1.4	-1.4	-1.4	-1.4
C(12)-C(16)	-2.15	-2.14	-2.12	-2.11	-2.09	-2.07
C(13)-C(14)	-2.26	-2.26	-2.26	-2.26	-2.26	-2.26
C(13)-H(13)	-1.73	-1.73	-1.73	-1.74	-1.74	-1.74
C(14)-C(15)	-1.29	-1.28	-1.28	-1.28	-1.29	-1.29
C(14)-H(14)	-1.74	-1.73	-1.73	-1.73	-1.73	-1.73
C(15)-C(16)	-1.29	-1.29	-1.3	-1.3	-1.31	-1.31
Ring Connectors						
C(6)-C(3)	-1.47	-1.47	-1.48	-1.49	-1.5	-1.51
C(9)-C(12)	-1.48	-1.49	-1.5	-1.51	-1.52	-1.54
Terminal						
C(15)-S(2)	-0.393	-0.394	-0.395	-0.395	-0.397	-0.398
C(1)-S(1)	-0.413	-0.415	-0.417	-0.418	-0.417	-0.416
S(2)-Au(2)	-0.163	-0.162	-0.16	-0.155	-0.15	-0.143
S(1)-Au(1)	-0.166	-0.166	-0.166	-0.165	-0.165	-0.165
C-H Bonds						
C(1)-H(1)	-1.6	-1.6	-1.6	-1.6	-1.61	-1.61
C(2)-H(2)	-1.73	-1.74	-1.74	-1.74	-1.74	-1.75
C(4)-H(4)	-1.73	-1.72	-1.72	-1.72	-1.72	-1.73
C(5)-H(5)	-1.74	-1.74	-1.75	-1.75	-1.76	-1.76
C(7)-H(7)	-1.72	-1.72	-1.73	-1.73	-1.73	-1.74
C(10)-H(10)	-1.72	-1.72	-1.72	-1.72	-1.71	-1.71

C(11)-H(11)	-1.72	-1.72	-1.73	-1.73	-1.73	-1.74
C(13)-H(13)	-1.73	-1.73	-1.73	-1.74	-1.74	-1.74
C(14)-H(14)	-1.74	-1.73	-1.73	-1.73	-1.73	-1.73
C(15)-H(15)	-1.68	-1.68	-1.68	-1.68	-1.68	-1.67
C(16)-H(16)	-1.73	-1.73	-1.74	-1.74	-1.74	-1.74

Atomic charges and Frontier molecular orbital analysis

The point charge distribution of molecules [12] should be well understood to explore the chemical reactivity of the molecule. The numerous studies reported that MK method provides the finest values according to electrostatic criteria. Hence, in this work, the point charges have been computed and related by MPA and MK schemes (Table8). The atomic charges are fitted to reflect the molecular electrostatic potential at a number of points around the molecule [13].

With an increase of the applied electric field, the MPA and NPA charges of all carbon atoms except that are bonded to sulphur atoms possess negative charge and differ with the increase of field. The C (1)atom holds a negative NPA and MPA charge, which varies from -0.513 to -0.532e and with the increase of the field, the charge of C (1) atom varies from -0.351 to -0.363e. The NPA charges of Au atom at the left end increases from 0.246 to 0.253e, as the field increases, unlikely at the right end it was decreased from 0.182 to 0.035e. The MPA charge for all the carbon atoms are found almost negative, and the H-atoms are positive for the zero field, with the increase of the field, the charges also increase. For the higher applied electric field, the MPA charge of sulphuratom at the left end increases steadily from 0.052 to 0.1e, while at the right end this effect is conflicting and the charge is increased from 0.046 to 0.052e. The charges of Au (1) atom increases from 0.246 to 0.253e, for higher fields but the same for Au (2), it was decreased from 0.182 to 0.035e.

Table No. 8:"Atomic charges(e) [First line: MPA; Second line: NPA] of Au and S substituted DCC for the zero and various applied EFs (VÅ^{-1})"
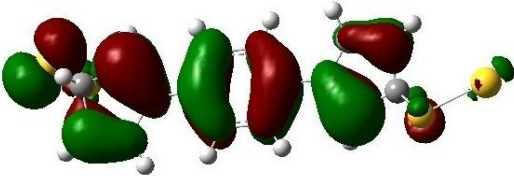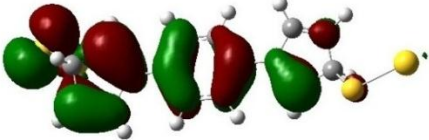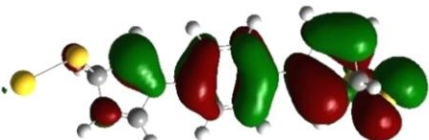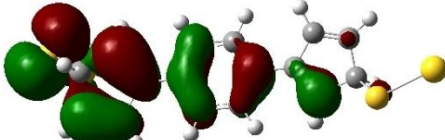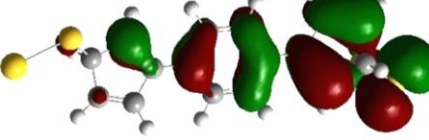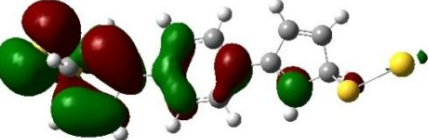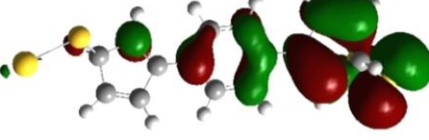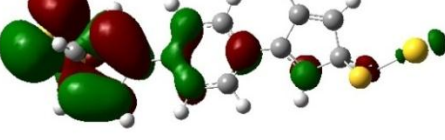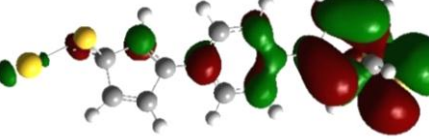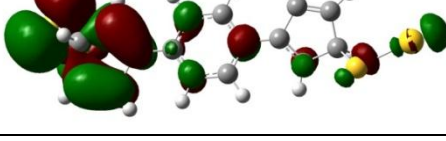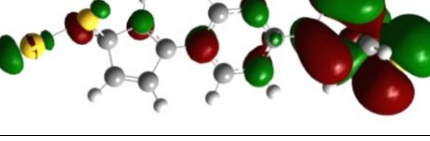
Atoms	Applied electric field					
	0	0.05	0.1	0.15	0.21	0.26
C(1)	-0.513	-0.517	-0.521	-0.526	-0.532	-0.532
	-0.351	-0.354	-0.357	-0.36	-0.363	-0.363
C(2)	-0.348	-0.344	-0.339	-0.333	-0.321	-0.321
	-0.192	-0.184	-0.175	-0.164	-0.149	-0.149
C(3)	0.329	0.328	0.328	0.327	0.326	0.326
	-0.058	-0.062	-0.066	-0.07	-0.073	-0.073
C(4)	-0.335	-0.337	-0.339	-0.34	-0.34	-0.34
	-0.219	-0.223	-0.226	-0.229	-0.231	-0.231
C(5)	-0.197	-0.193	-0.19	-0.185	-0.182	-0.182
	-0.193	-0.189	-0.184	-0.179	-0.175	-0.175
C(6)	0.369	0.37	0.371	0.372	0.373	0.373
	-0.05	-0.043	-0.036	-0.029	-0.022	-0.022
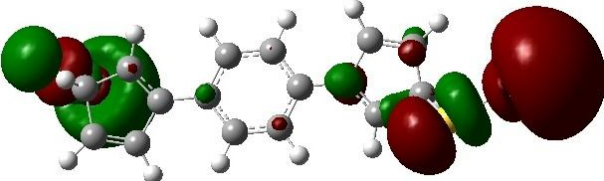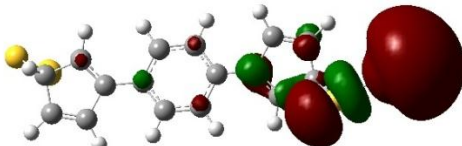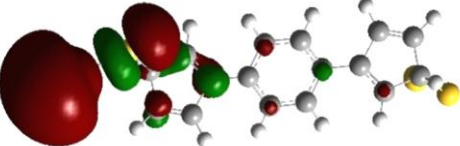
C(7)	-0.39	-0.389	-0.388	-0.386	-0.382	-0.382
	-0.183	-0.183	-0.183	-0.182	-0.18	-0.18
C(8)	-0.381	-0.38	-0.378	-0.376	-0.376	-0.376
	-0.188	-0.187	-0.186	-0.185	-0.184	-0.184
C(9)	0.362	0.362	0.362	0.362	0.364	0.364
	-0.057	-0.062	-0.067	-0.071	-0.073	-0.073
C(10)	-0.389	-0.388	-0.387	-0.386	-0.386	-0.386
	-0.179	-0.178	-0.177	-0.175	-0.174	-0.174
C(11)	-0.381	-0.381	-0.381	-0.381	-0.379	-0.379
	-0.192	-0.192	-0.192	-0.192	-0.191	-0.191
C(12)	0.326	0.327	0.328	0.328	0.327	0.327
	-0.039	-0.033	-0.027	-0.022	-0.019	-0.019
C(13)	-0.353	-0.35	-0.347	-0.344	-0.341	-0.341
	-0.219	-0.215	-0.212	-0.21	-0.208	-0.208
C(14)	-0.136	-0.138	-0.141	-0.145	-0.148	-0.148
	-0.179	-0.181	-0.183	-0.184	-0.184	-0.184
C(15)	-0.486	-0.485	-0.484	-0.484	-0.483	-0.483
	-0.334	-0.332	-0.331	-0.33	-0.329	-0.329
C(16)	-0.392	-0.394	-0.395	-0.395	-0.394	-0.394
	-0.204	-0.209	-0.214	-0.217	-0.218	-0.218
S(2)	0.046	0.05	0.053	0.054	0.052	0.052
	-0.168	-0.16	-0.154	-0.149	-0.148	-0.148
S(1)	0.052	0.064	0.076	0.088	0.1	0.1
	-0.177	-0.167	-0.158	-0.149	-0.142	-0.142
Au(2)	-0.071	-0.098	-0.128	-0.163	-0.205	-0.205
	0.182	0.153	0.121	0.082	0.035	0.035
Au(1)	-0.017	-0.018	-0.018	-0.016	-0.01	-0.01
	0.246	0.245	0.244	0.245	0.253	0.253
Ring 2						
H(7)	0.223	0.226	0.229	0.231	0.232	0.234
	0.218	0.219	0.221	0.222	0.224	0.225
H(11)	0.22	0.223	0.225	0.228	0.229	0.231
	0.216	0.217	0.219	0.22	0.222	0.223
H(10)	0.227	0.225	0.223	0.221	0.221	0.22
	0.219	0.218	0.217	0.216	0.216	0.216
H(8)	0.222	0.22	0.218	0.217	0.216	0.215
	0.216	0.215	0.214	0.214	0.213	0.213
Ring 3						
H(13)	0.237	0.239	0.24	0.241	0.242	0.243

	0.221	0.222	0.223	0.223	0.224	0.224
H(14)	0.237	0.235	0.234	0.232	0.231	0.231
	0.224	0.223	0.222	0.221	0.22	0.219
H(15)	0.285	0.283	0.281	0.278	0.275	0.272
	0.268	0.266	0.264	0.262	0.261	0.259
H(16)	0.251	0.252	0.252	0.253	0.254	0.253
	0.225	0.226	0.227	0.227	0.228	0.228
Ring 1						
H(2)	0.245	0.246	0.246	0.247	0.248	0.25
	0.224	0.224	0.224	0.224	0.224	0.225
H(1)	0.275	0.279	0.284	0.288	0.294	0.301
	0.276	0.279	0.282	0.285	0.288	0.292
H(5)	0.247	0.251	0.254	0.258	0.262	0.267
	0.228	0.23	0.233	0.236	0.239	0.242
H(4)	0.235	0.234	0.233	0.232	0.232	0.232
	0.22	0.219	0.219	0.218	0.218	0.219

The energy gap between the highest occupied molecular orbital (HOMO) and lowest unoccupied molecular orbital (LUMO) is called as the HOMO-LUMO gap (HLG), which governs the charge transport properties of the molecule [14].Fig.5 shows the molecular orbital for the zero and higher levels of the applied electric field for DCC molecular wire. The symmetric variations were observed in HOMO and LUMO level for the reverse applied electric fields. The HLG decreases from 2.07 to 0.70eV for the applied field (0.00 - 0.26 $V\mathring{A}^{-1}$).

The density of states (DOS) for the zero and higher applied field (0.26 $V\mathring{A}^{-1}$) are depicted in Fig (6-11), in which the green solid lines specifies the HOMO and the blue reflects the LUMO.The DOS spectrum clearly shows that the hybridization of the molecular level with that of the gold atom expands the DOS peaks. The DOS peaks at 0.05 $V\mathring{A}^{-1}$, are in minima, directs the discrete molecular level with a homo-lumo gap of 1.79eV. With the increase of electric field from 0.10 to 0.26 $V\mathring{A}^{-1}$, the gap between HOMO and LUMO levels were found to be shortened from 1.45 to 0.70eV.

EF(VÅ^{-1})	HOMO	
0.00		
	Positive field	Negative field
0.05		
0.10		
0.15		
0.21		
0.26		

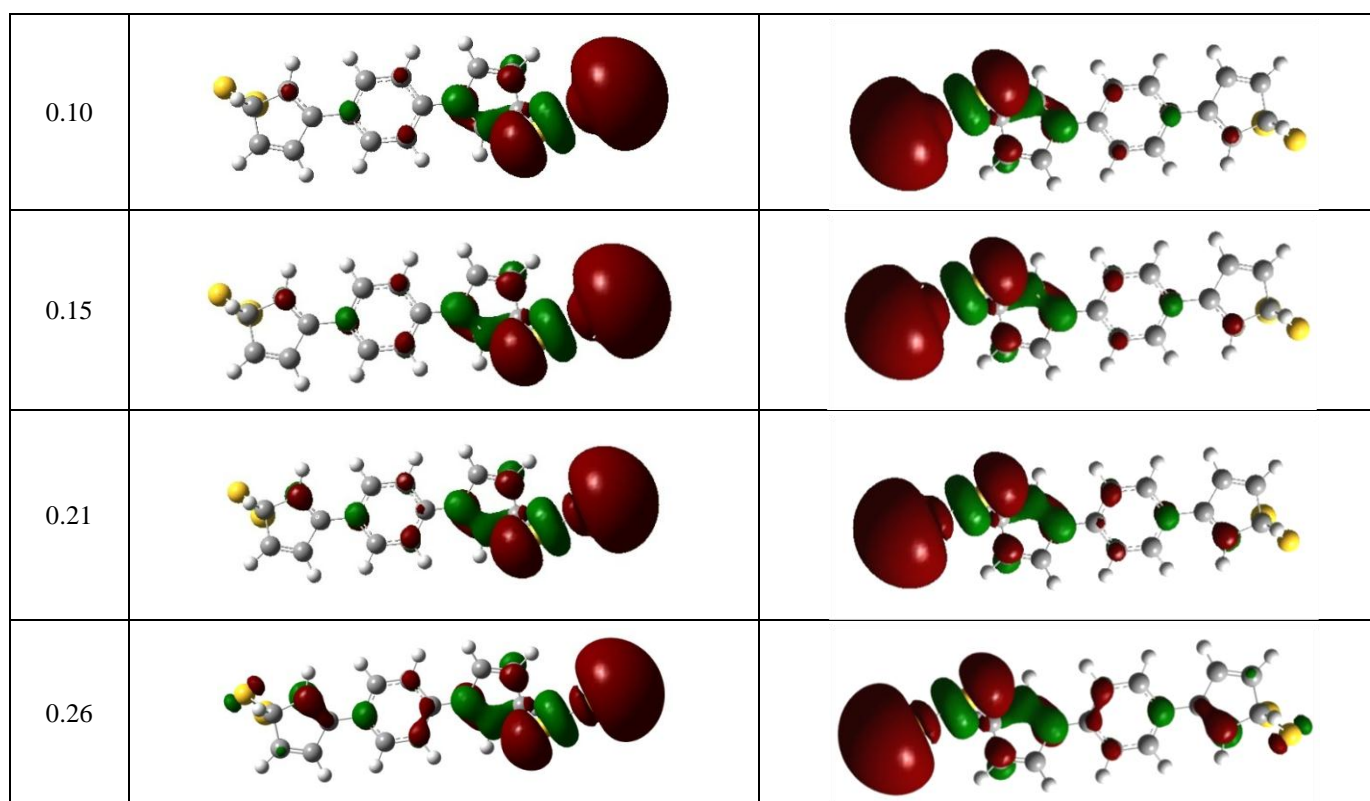| EF VÅ^{-1}	LUMO	
0.00		
	Positive field	Negative field
0.05		

0.10		
0.15		
0.21		
0.26		

Figure. 5 - Isosurface representation of molecular orbitals of Au and S substituted DCC for the zero and various applied EFs, which are drawn at 0.05 au surface values

The energy level variations of the molecule are nearly symmetric for both positive as well as negative bias, and thus the conductivity of the DCC molecular wire is irrespective of the direction of the external applied electric field. The narrow HLG enables the large electron conduction along the molecule[15], hence, the Au substituted DCC molecular wire can turn as a competent molecular nanowire. Fig. 12exemplifies the energy levels of the molecule for applied electric fields.
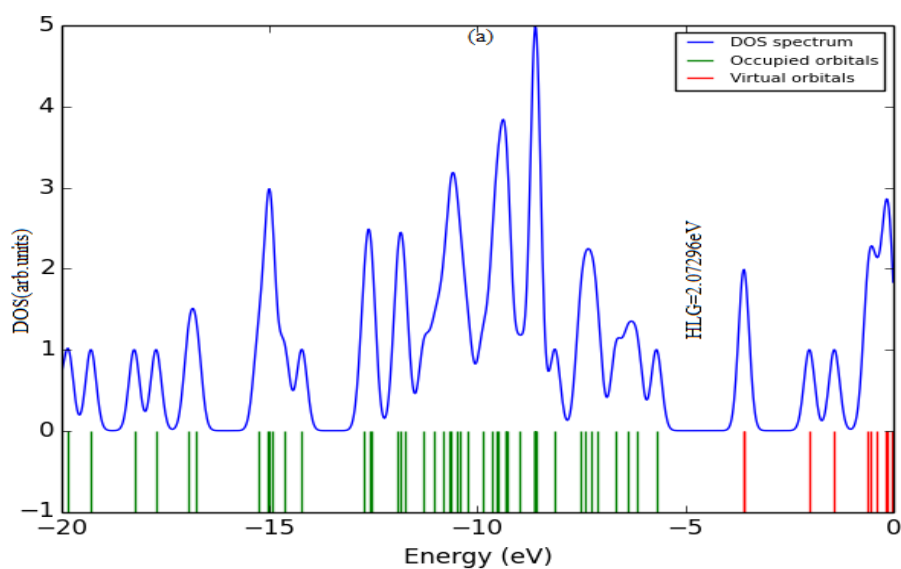
Figure 6 - DOS pectrum of DCC for zero field.
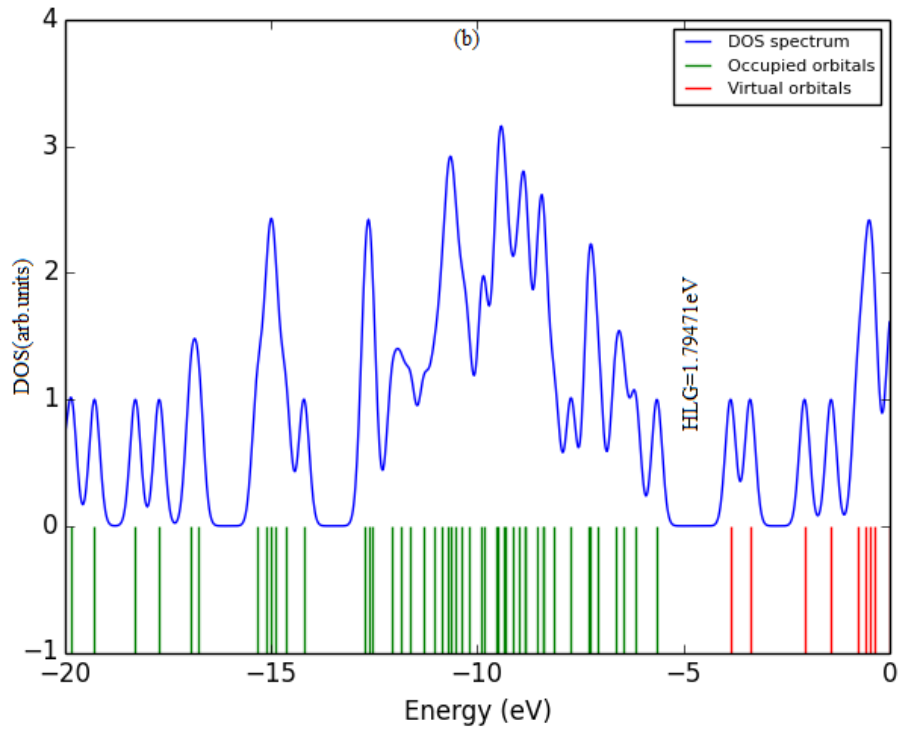
Figure.7 DOS Spectrum of DCC for the applied field 0.05 VÅ^{-1}.
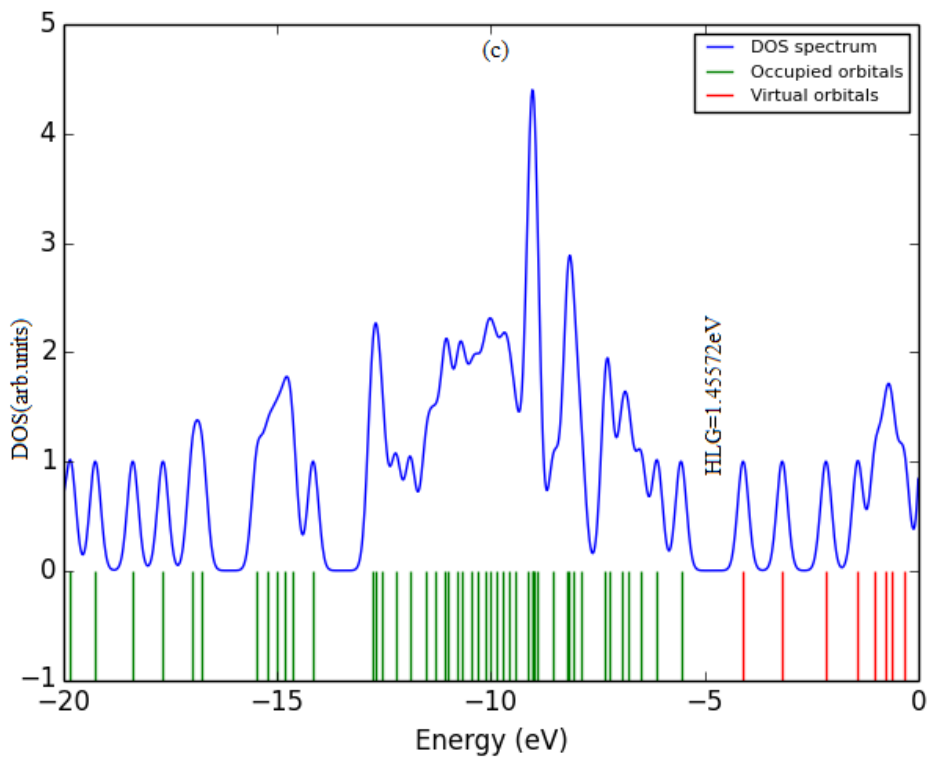
Figure.8- DOS Spectrum of DCC for for the applied field 0.10 VÅ^{-1}.
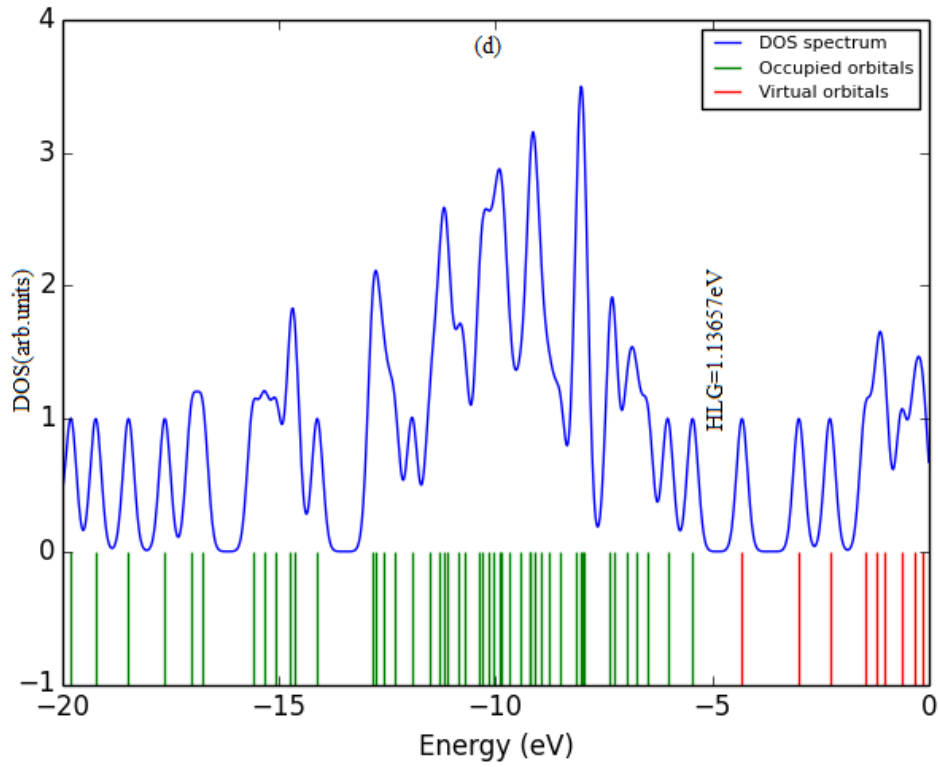
Figure.9 - DOS Spectrum of DCC for zero for the applied field 0.15 VÅ⁻¹.

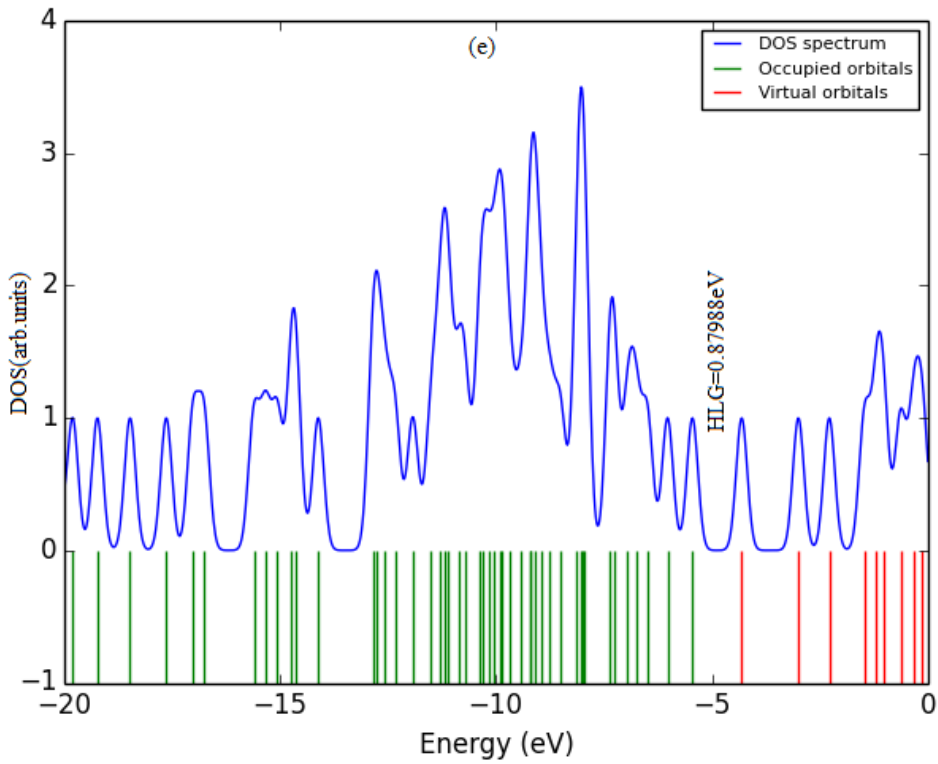
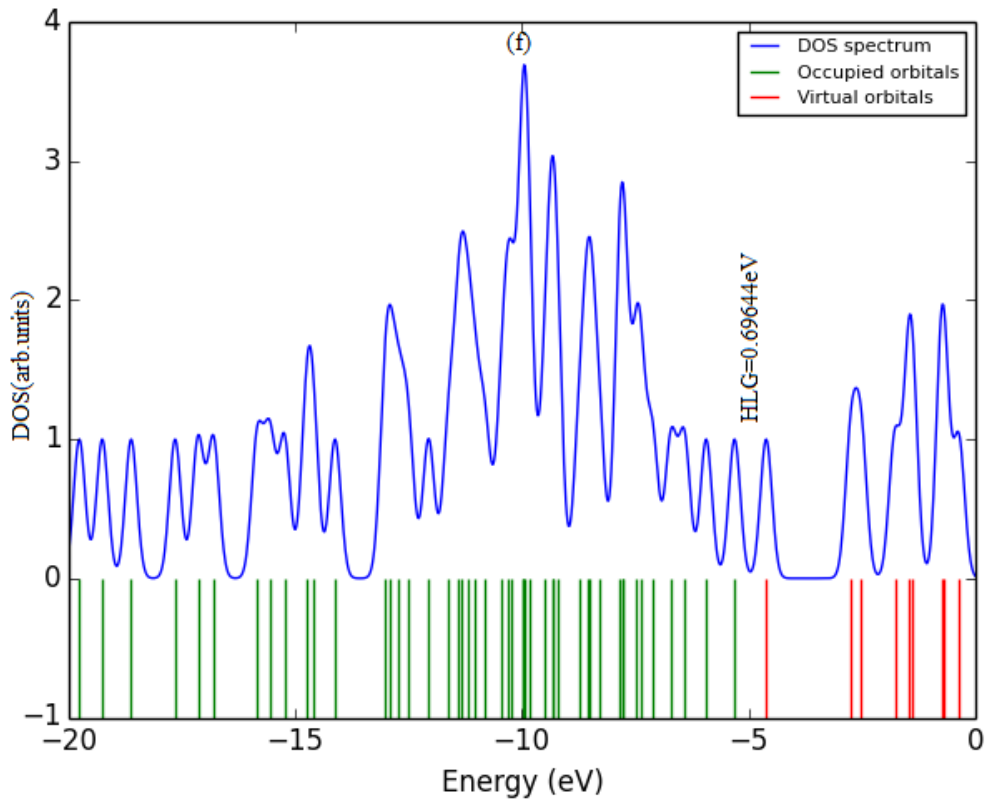**Figure.10- DOS Spectrum of DCC forfor the applied field 0.21 VÅ⁻¹.**

Figure. 11- DOS Spectrum of DCC for for the applied field 0.26 VÅ⁻¹.

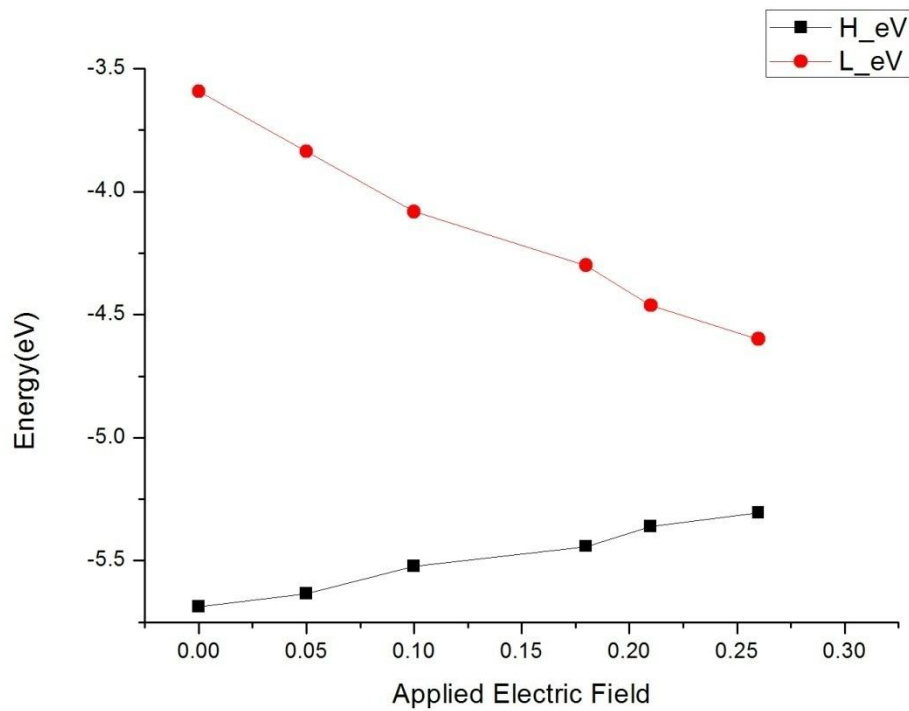**Figure.12- Energy levels ofAu and S substituted DCC for the zero and various applied EFs.**

Electrostatic potential

The charged regions of the molecules were able to locate from the electrostatic potential (ESP) surface of the molecule. Fig. 13depicts the is surface illustration of ESP of DCC molecule, in which the Au−S bond regions reveals the high negative electrostatic potential. The potential surface plot displays the charged regions of the DCC molecular wire, and it obviously replicates the contrasting influences from the nuclei and the electrons [16]. The negative potential is mounted over the S-atoms for the zero applied field, which is pivoted at right and left ends of the molecule and the rest of the molecule have positive electrostatic potential. When the applied electric field is increased from 0 to 0.15 VÅ^{-1}, the negative electrostatic potential at the left enddiminutes for each field step and it completely dissolves at the right end, the negative electrostatic potential increases and extends around the right edge of the molecule. Further escalation of the electric field to 0.26 VÅ^{-1}, the negative electrostatic potential was extentcompletelyabout the right end of the molecule, which specifies that as the electric field increases the charge was found to migrate from left to right end of the DCC molecular wire. Likewise, when the field is reversed, the negative electrostatic potential regions are drifted from right to the left end of the DCC molecule.

Ef	Electrostatic Potential	
0.00		
	Positive field	Negative field
0.05		
0.10		
0.15		
0.21		

| 0.26 | | |

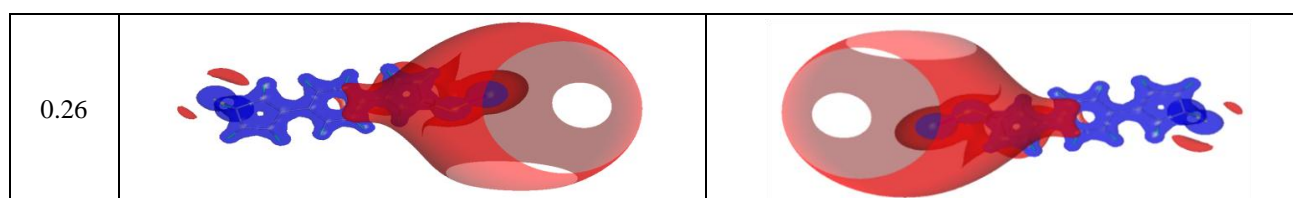**Figure.13 - Electrostatic potentials ofAu and S substituted DCC for the zero and various applied EFs. Blue: positive potential (0.5 eÅ^{-1}), Red: negative potential (-0.04 eÅ^{-1}).**
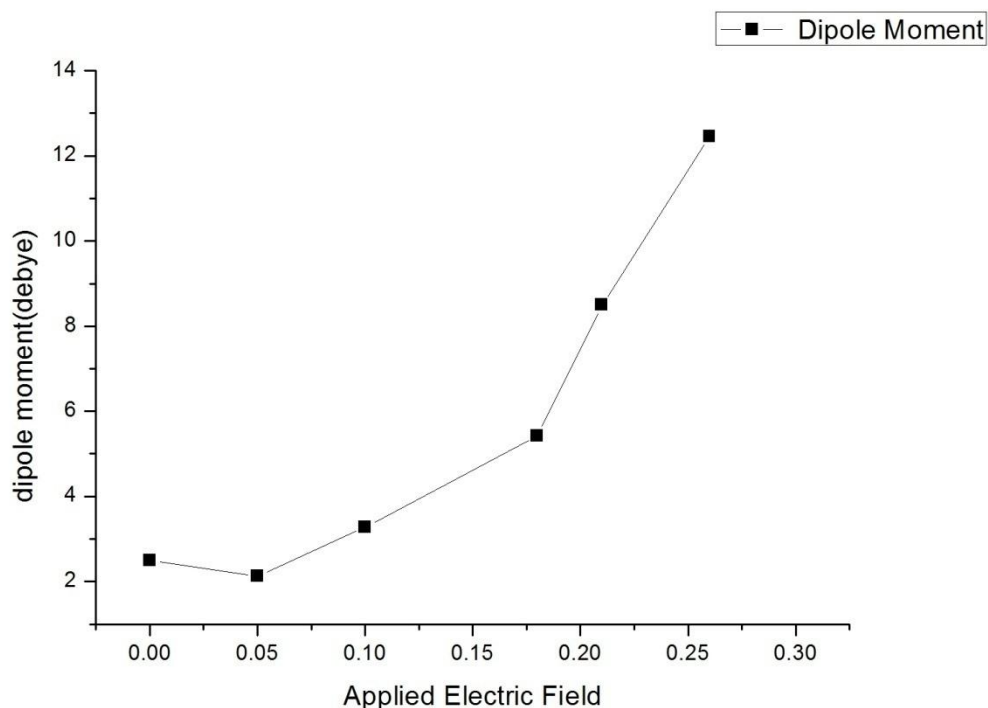
Molecular dipole moment

Figure.14- Variation of the molecular dipole moment of Au and S substituted DCC for various applied EFs

When the molecule is exposed to the external applied electric field, the molecule gets polarized, which brings the change in the dipole moment of the molecule. Hence, it is vital to regulate the dipole moment of the molecule for the applied electric field. Lately, Kirtman et al.,[17]examined the deviations of the molecular dipole moment for the numerous applied electric field and noticed a linear nature. However, this linearity no longer subsists beyond some specified applied electric field and it is insignificant since no molecular electronic device functions under such high voltages. Here, the dipole moment of the DCC molecular wire for zeroand non-zero applied electric field has been computed.

The disparity of the molecular dipole moment for the external applied electric field is depicted in Figure14. The molecular dipole moment is 2.50Debye for zero fields, and the variation is found to be linear with the applied external electric field. It was noticed that the molecule becomes

highly polarized for the field, 0.26 VÅ^{-1}; this polarization convinces to have high molecular dipole moment value of about 12.45Debye. As reported by Rai*et al*, furtherrisingthe applied electric field, the "high voltage" may establish to warrant the nonlinear variations in the dipole moment.

I–V characteristic curve

The current-voltage characteristic (i.e) I-V characteristic curve is commonly used to regulate the basic factors of electronic devices [18]. In this analysis, the I-V characteristics (Fig. 15) of the DCC molecular wire have been assessed using the Landauer formula. The tunneling electric current (I) has been computed for the various applied electric field. The resistance (R) and the linear conductance (G) can be represented as

$$R = G^{-1} = (12.91 \text{ K}\Omega)/ T_l T_r T_m \quad ....(1)$$

Where T_l and T_r are the charge transport efficiency in the left and right end contacts and T_m is the electron transmission through the molecule and it can be expressed as

$$T_m = \exp(-\beta L) \quad .....(2)$$

here L is the molecular length and β is the tunneling decay factor which can be calculated by

$$\beta = (1/\hbar) [2m^*\alpha \phi]^{1/2} .....(3)$$

where m* is the effective mass of the electron, α is the symmetry parameter of potential profile[19] and ϕ is the potential barrier height for tunneling through the highest occupied orbital or the lowest unoccupied orbital level. For an applied electric fieldϕ is half of the HOMO-LUMO gap.
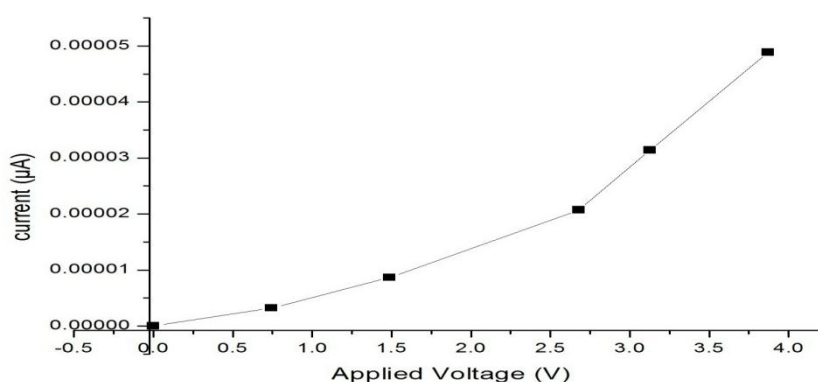

Figure. 15 - I-V characteristics of DCC molecule for various applied EFs.

The resistance of the DCC molecular wire wasdeliberate from the above equation (1). The voltage (V) across the molecule of length L has been computed from the equation V = EL. Figure 10 shows the I-V characteristics of DCC wire, and it was noticed that the current I increases in a non-linear manner with theapplied electric field.

CONCLUSION

This sectionpronouncesthe structural confirmation, topological properties of electron density via QTAIM and the electrical characteristics of gold and sulphur substituted DCCmolecular nanowire for externally applied fields ranges from 0to ±0.26 VÅ^{-1}from DFT method along with LANL2DZ basis set.The Au−S bond length at the right end is found slightly longer than the left end for the applied field; this dissimilaritymight be due to the Au atom at the L-end having themaximum electric field than the same at the right end. Further, the geometry analysisfor all the electric fieldobviously shows the left and right end groups are very sensitive to the applied electric field, while the mid portion ofDCC is almost unaffected to the electric field. The analysis of bond topologydisclosesthat the deviation in electron density $\rho_{bcp}(r)$ and $\nabla^2\rho_{bcp}(r)$ at the bond critical points of all the bonds for zero and the higher electric fields, it was noted that variations are feeble and found to be systematic. As for the molecular orbital concern, HOMO and LUMO levels are approached each other for increasing electric field. The hybridization of the molecular levels widens the density of states whichdecreases the HOMO-LUMO gap from 2.09 to 0.70eVforthe increases in the applied field. The current-voltage curve seems very symmetric for the current flow in both directions through the molecule and it obviously shows the presence of nonlinear behavior of DCC molecular wire. The applied electric field polarizes the DCC molecule, as a result, the dipole moment of the molecule rises from 2.50 to 12.45 D. On the whole, the terminal groups of the DCC are responding very well towards the applied electric field.

REFERENCES

1. Srinivasan P, Stephen AD, Kumaradhas P. Effect of gold atom contact in conjugated system of one-dimensional octane dithiolate based molecular wire: A theoretical charge density study. *J Mol Struct THEOCHEM*. 2009;910(1-3):112-121. doi:10.1016/j.theochem.2009.06.026

2. Gollis MH, Belenyessy LI, Gudzinowicz BJ, Koch SD, Smith JO, Wineman RJ. Evaluation of Pure Hydrocarbons as Jet Fuels. *J Chem Eng Data*. 1962;7(2):311-316. doi:10.1021/je60013a044

3. Biegler-könig FW, Bader RFW, Tang T-H. Calculation of the average properties of atoms in molecules. II. *J Comput Chem*. 1982;3(3):317-328. doi:10.1002/jcc.540030306

4. Frisch MJ, Trucks GW, Schlegel HB, et al. Gaussian09 Revision D.01, Gaussian Inc. Wallingford CT. *Gaussian 09 Revis C01*. 2010. doi:10.1017/CBO9781107415324.004

5. Yang Y, Weaver MN, Merz KM. Assessment of the "6-31+G** + LANL2DZ" Mixed Basis Set Coupled with Density Functional Theory Methods and the Effective Core Potential: Prediction of Heats of Formation and Ionization Potentials for First-Row-Transition-Metal Complexes. *J Phys Chem A*. 2009;113(36):9843-9851. doi:10.1021/jp807643p

6. König FB, Schönbohm J, Bayles D. AIM2000-a program to analyze and visualize atoms in molecules. *J Comput Chem*. 2001. doi:10.1002/1096-987X(20010415)22

7. O'Boyle NM, Tenderholt AL, Langner KM. Cclib: A library for package-independent computational

chemistry algorithms. *J Comput Chem*. 2008. doi:10.1002/jcc.20823

8. Schnabel A, Ahmadi-Simab K, Gross WL. Lungenbeteiligung beisystemischenVaskulitiden. *Atemwegs- und Lungenkrankheiten*. 2007;33(01):2-13. doi:10.5414/atp33002

9. Di Ventra M, Pantelides ST, Lang ND. The benzene molecule as a molecular resonant-tunneling transistor. *Appl Phys Lett*. 2000. doi:10.1063/1.126673

10. Cremer D, Kraka E. Theoretical Determination of Molecular Structure and Conformation. 15. Three-Membered Rings: Bent Bonds, Ring Strain, and Surface Delocalization. *J Am Chem Soc*. 1985. doi:10.1021/ja00299a009

11. Gibbs G V, Tamada O, Boisen MB, Hill FC. Laplacian and bond critical point properties of the electron density distributions of sulfide bonds; a comparison with oxide bonds. *Am Mineral*. 1999;84(3):435-446. doi:10.2138/am-1999-0328

12. Murray JS, Politzer P. The electrostatic potential: An overview. *Wiley Interdiscip Rev Comput Mol Sci*. 2011. doi:10.1002/wcms.19

13. Reed AE, Weinstock RB, Weinhold F. Natural population analysis. *J Chem Phys*. 1985. doi:10.1063/1.449486

14. Davis WB, Svec WA, Ratner MA, Wasielewski MR. Molecular-wire behaviour in p -phenylenevinylene oligomers. *Nature*. 1998;396(6706):60-63. doi:10.1038/23912

15. Lu J-Q, Wu J, Chen H, Duan W, Gu B-L, Kawazoe Y. Electronic transport mechanism of a molecular electronic device: structural effects and terminal atoms. *Phys Lett A*. 2004;323(1-2):154-158. doi:10.1016/j.physleta.2004.01.055

16. Rai D, Kulkarni AD, Gejji SP, Pathak RK. Water clusters (H2O)n, n=6−8, in external electric fields. *J Chem Phys*. 2008;128(3):34310. doi:10.1063/1.2816565

17. Kirtman B, Champagne B, Gu FL, Bishop DM. Coupled-perturbed Hartree-Fock treatment of infinite periodic systems: Application to static polarizabilities and hyperpolarizabilities of polydiacetylene, polybutatriene, and interacting pairs of polyacetylene chains. *Int J Quantum Chem*. 2002;90(2):709-718. doi:10.1002/qua.951

18. Kushmerick JG, Naciri J, Yang JC, Shashidhar R. Conductance Scaling of Molecular Wires in Parallel. *Nano Lett*. 2003;3(7):897-900. doi:10.1021/nl034201n

19. Farmanzadeh D, Ashtiani Z. Theoretical study of a conjugated aromatic molecular wire. *Struct Chem*. 2010;21(4):691-699. doi:10.1007/s11224-010-9599-5